DIAS-STP-06-11

Numerical simulations of a non-commutative theory: the scalar model on the fuzzy sphere

Marco Panero

School of Theoretical Physics
Dublin Institute for Advanced Studies
10 Burlington Road
Dublin 4, Ireland

e-mail: panero@stp.dias.ie

Abstract

After reviewing the construction of the fuzzy sphere and the formulation of the scalar theory in this non-commutative setting, we address a detailed non-perturbative study by means of a novel algorithm, which strongly reduces the correlation problems in the matrix update process, and which allows the investigation of different regimes of the model in a precise and reliable way. We study the modes associated to different momenta and the rôle they play in the case when the potential admits classically degenerate minima, pointing out a consistent interpretation which is corroborated by our data, and which sheds further light on the results obtained in some previous works. We also investigate the effects of the non-commutative anomaly predicted in a one-loop perturbative analysis of the model, which is expected to induce a distortion of the dispersion relation on the fuzzy sphere.

1 Introduction

The study of quantum field theory in non-commutative spaces has attracted considerable attention over the last years [1–4]. This research area has a long history, since the possibility of a quantised structure of spacetime at short distances was first mentioned as early as in the 1930's in some correspondence among Heisenberg, Peierls, Pauli and Oppenheimer [5, 6], and in the papers published by Snyder [7], by Yang [8] and by Moyal [9] during the 1940's. Although the original motivation to use non-commutativity as a tool to regularise QFT was soon frustrated — while the renormalisation approach proved to be a successful method to handle the divergences encountered in the formulation in commutative spacetime —, a renewed interest in non-commutative spaces has arisen again in more recent years, with the application of this formalism to solid-state physics and to the problem of the quantum Hall effect [10], and with the discovery of the relevance of such spaces to string theory [11–14] and to a possible quantum theory of gravity [15].

At present, the Groenewold-Moyal $\mathbb{R}^n_\theta$ spaces are probably the most extensively studied non-commutative spaces. The issues related to renormalisability, causality, non-locality, Poincaré invariance of QFT in these spaces have been addressed in several works [16–32]; a lattice-like regularised formulation has also allowed to investigate numerically various aspects of these models [33–41]. In particular, one of the most interesting — albeit troublesome — features is the fact that the effective action describing QFT in a Groenewold-Moyal space is divergent when the external momentum along the non-commutative directions vanishes: this effect arises from the integration of the high-energy modes in non-planar loop diagrams, and is henceforth called "ultra-violet/infra-red (UV/IR) mixing".

Another class of non-commutative spaces is given by fuzzy spaces: they are built approximating the infinite-dimensional algebra of functions on some particular manifold by means of a finite-dimensional algebra of matrices. Under some conditions, this construction is possible for even-dimensional co-adjoint orbits of Lie groups which are symplectic manifolds — see [42–48] and references therein. In particular, co-adjoint orbits of semi-simple Lie groups are adjoint orbits; examples include the $\mathbb{C}P^n$ complex projective spaces, for $n \leq 3$. The most-widely known example of a fuzzy space is the fuzzy two-sphere S^2_F [42], built truncating the algebra of functions on the commutative sphere S^2 to a maximum angular momentum $l_{\max}$. The fuzzy sphere depends on two parameters: the matrix size $N = l_{\max} + 1$ and the radius R; it is possible to show that the commutative sphere and the non-commutative plane can be obtained in different limits of N and R.

A one-loop perturbative calculation shows that, for every finite N, QFT on the fuzzy sphere is finite and not affected by the UV/IR mixing problem [49] (although — due to a non-commutative anomaly — the latter re-emerges once the limit is taken, in which the fuzzy sphere goes over to the non-commutative plane $\mathbb{R}^2_\theta$). This feature, as well as the fact that the fuzzy approach explicitly preserves the symmetries of the original manifold for any value of N and allows a well-defined treatment of the topological properties [50–56] has led to suggest the fuzzy space a potentially interesting candidate for regularisation of quantum field theory.

As a matter of fact, QFT on the fuzzy sphere is mathematically well-defined and finite [57], and the formulation is amenable to a non-perturbative approach and to numerical studies using

Monte Carlo simulations, with fields represented as finite-dimensional matrices. This approach has been followed in various recent works [58–64].

In the present paper we address a detailed Monte Carlo study of the Φ^4 scalar field theory on the fuzzy sphere; among other issues of interest, this simple model provides a laboratory to test the possibility to use the fuzzy space approach as a potential regularisation scheme for more realistic field theories. As it concerns the practical implementation of Monte Carlo simulations of the model, we shall present a novel algorithm, which reduces the autocorrelation time, combining overrelaxation steps with ergodic configuration updates.

This manuscript has the following structure: in section 2 the theoretical framework underlying the model is recalled, and the basic notations are introduced; in section 3 we discuss the implementation of the numerical simulations of the model, and present the results obtained with our algorithm. In section 4 we comment on the implications of these results, whereas section 5 is devoted to some concluding remarks and possible research perspectives. A technical discussion of the algorithm is presented in the Appendix A.

2 Review of the construction of the model

A general discussion of the mathematical construction of fuzzy spaces can be found in many excellent articles and books, like, for instance [48]; for the scalar field theory on the fuzzy sphere S_F^2, we refer the reader to the detailed presentation in [57], which we summarise below.

The infinite-dimensional, commutative algebra of polynomials generated by the $\{x_i\}_{i=1,2,3}$ coordinates on the two-dimensional sphere $x_i x_i = R^2$ embedded in $\mathbb{R}^3$ is replaced by a non-commutative algebra generated by $\{\hat{x}_i\}_{i=1,2,3}$ operators satisfying:

$$[\hat{x}_i, \hat{x}_j] = \frac{2R}{\sqrt{N^2-1}} i\epsilon_{ijk}\hat{x}_k \ , \tag{1}$$

$$\sum_{i=1}^{3} \hat{x}_i^2 = R^2 \ ; \tag{2}$$

therefore the $\{\hat{x}_i\}_{i=1,2,3}$ operators obey — modulo a trivial rescaling — the $su(2)$ Lie algebra.

The relations above can be realised using the Wigner-Jordan construction of the $su(2)$ generators, and restricting to the finite-dimensional (N-dimensional) subspace of the Fock space generated by the creation operators.

Accordingly, the algebra of functions on the commutative sphere S^2 is replaced by the Mat_N algebra, whose elements can be expanded into irreducible representations of $su(2)$.

Integrals of functions on the commutative sphere are replaced by the matrix trace operation, which is invariant under the adjoint action of $su(2)$, and an inner product on S_F^2 can be defined as:

$$\langle \Phi, \Psi \rangle = \frac{4\pi R^2}{N} \mathrm{tr}\left(\Phi^\dagger \Psi\right) \ . \tag{3}$$

The vectors describing derivations on the commutative sphere are mapped to the adjoint action

of the $\{L_i\}_{i=1,2,3}$ generators of the $su(2)$ algebra on S_F^2:

$$[L_i, \Phi] \ . \tag{4}$$

A convenient basis for the Mat_N algebra is provided by the polarisation tensors $\{\hat{Y}_{l,m}\}$ (with: $0 \leq l \leq N-1$, $-l \leq m \leq l$) satisfying:

$$\left[L_i, \left[L_i, \hat{Y}_{l,m}\right]\right] = l(l+1)\hat{Y}_{l,m} \ , \tag{5}$$

$$\left[L_3, \hat{Y}_{l,m}\right] = m\hat{Y}_{l,m} \ , \tag{6}$$

and the natural mapping to the spherical harmonics enjoying analogous properties offers a straightforward visualisation of S_F^2 as an approximation scheme for functions on the ordinary sphere. It is obvious, but important, to note that the fusion rules in the finite N case are different with respect to the commutative setting.

With this geometrical construction, the fuzzy sphere admits the commutative sphere S^2 and the Groenewold-Moyal plane $\mathbb{R}_\theta^2$ as two different limits: the former is recovered for $N \to \infty$ with R fixed, whereas the latter can be obtained — at least locally — via a stereographic projection from a fixed point, in the double limit: $N \to \infty$, $R \to \infty$, keeping R^2/N fixed. Here and in the following, we shall mainly concentrate on the finite radius case, and assume $R = 1$.

Having reviewed the construction of the fuzzy sphere, we can now define the action for a massive, neutral, scalar field with quartic interactions — according to the conventions used in [58] — as:

$$S = \frac{4\pi}{N}\mathrm{tr}\left(\Phi\left[L_i, [L_i, \Phi]\right] + r\Phi^2 + \lambda\Phi^4\right) \ , \tag{7}$$

where $\Phi \in \mathrm{Mat}_N$ is hermitian and depends on N^2 (real) degrees of freedom; it can be expanded in the $\{\hat{Y}_{l,m}\}$ basis as:

$$\Phi = \sum_{l=0}^{N-1} \sum_{m=-l}^{l} c_{l,m}\hat{Y}_{l,m} \tag{8}$$

and the $c_{l,m}$ coefficients can be considered as the dynamical degrees of freedom. They are complex numbers satisfying: $\bar{c}_{l,m} = (-1)^m c_{l,-m}$.

The model can be quantised in the path integral approach, defining the expectation values of generic observables $\mathcal{O} = \mathcal{O}(c_{l,m})$ as:

$$\langle \mathcal{O} \rangle = \frac{\int \Pi_{l,m} dc_{l,m} \mathcal{O}(c_{l,m}) e^{-S}}{\int \Pi_{l,m} dc_{l,m} e^{-S}} \ , \tag{9}$$

which can be evaluated perturbatively, or estimated numerically from Monte Carlo simulations.

The perturbative treatment of the theory can be formulated via a proper definition of the Feynman rules — in particular, the interaction vertices are modified in a non-trivial way, which depends on N, and is consistent with the fusion rules. A careful one-loop analysis of this model [49] shows that the UV/IR mixing phenomenon does not occur on S_F^2; however, a non-commutative

anomaly shows up, as a finite difference between planar and non-planar tadpole diagrams. This anomaly is expressed by a rotationally invariant, non-local contribution to the quantum effective action, and it has the following implications on the limits discussed above:

1. the anomaly survives the process of taking the limit to the commutative sphere. This seriously threatens the possibility to consider the fuzzy approach as a *bona fide* regularisation scheme for theories defined in a commutative space; however, according to [65], the problem may be overcome, redefining the interaction term in the matrix action with a normal-ordering prescription, which allows to cancel the undesired momentum-dependent quadratic terms in the effective action. An alternative, and more general, possibility would be to include rotationally symmetric higher derivative terms in the action, as suggested in [66].

2. On the other hand, when the Groenewold-Moyal plane limit is taken, the non-commutative anomaly reproduces the logarithmic divergence which is characteristic of the UV/IR mixing [23].

Strictly speaking, the Φ^4 scalar field theory on the commutative sphere with finite radius does not possess different phases; the two degenerate minima of the classical action in the $r < 0$ regime are connected by quantum tunneling effects, with a finite energetic amount required to switch between each other. It is worth remarking that from the point of view of the path integral approach to the quantum description for the theory — or for a regularised version thereof, which a correct numerical simulation should mimic — the tunneling process may be mediated by finite action configurations which are not spherically symmetric; in general, these configurations yield a non-negligible contribution to the path integral, and their signature in the numerical results will show up through non-vanishing expectation values for the modes above the scalar channel. Clearly, this is an effect which, *in se*, has nothing to do with non-commutativity; it should be properly taken into account when discussing the numerical results obtained from simulations on the fuzzy sphere.

On the other hand, the non-commutativity intrinsic to the fuzzy regularisation may give rise to further non-trivial effects, and possibly induce qualitative changes in the quantum dynamical behaviour of the model: the most striking example is the non-commutative anomaly [49], which distorts the dispersion relation for a scalar field with square mass $\mu^2 = r > 0$.

The real scalar model with quartic interactions on the fuzzy sphere was studied numerically in [58, 59]; there it was claimed that the model exhibits three different phases: a disordered phase, in which the field typically fluctuates around zero; a uniform order phase, characterised by fluctuations around the broken-symmetry minima of the potential, and a non-uniform order phase, which was described as new, intermediate, phase, intrinsically related to the matrix nature of the fuzzy regularisation. The appearance of the latter was interpreted assuming that, in a certain parameter range, the kinetic contribution to the action might be negligible, and the dynamics of the system were effectively reduced to the framework of a pure potential model [67, 68]. This phase was also described as analogous to the striped phase predicted in [25] for non-commutative Groenewold-Moyal spaces, and observed numerically in [38].

Having reviewed the construction of the model and the results of previous studies, we can now focus on the issues that will be the main subject of the numerical investigation described in section 3; in particular, we shall consider both the $r < 0$ and $r > 0$ regimes, focusing on different aspects which are relevant to the two cases:

- in the $r < 0$ regime, the average values of the square norms of the $c_{l,m}$ coefficients and their dependence on r encode the information about the rôle played by the channels associated to different momenta; in order to look for (approximate) transitions among different regimes, the trace susceptibility can be used, as it describes the fluctuations associated to the scalar mode. The contributions to the action from the kinetic term and from the potential term can be studied separately, in order to investigate the relevance of the so-called "pure potential model" [67, 68] to the dynamics of the system.

- In the $r > 0$ regime, which — in principle — could provide a regularised version of the field theory of a massive, scalar particle on the commutative sphere, a non-commutative anomaly has been shown to arise [49]; this anomaly modifies the dispersion relation in a non-trivial way.

These issues are discussed in more detail below.

3 Numerical simulations

The numerical approach to the model is completely straightforward, and, under many respects, analogous to the lattice setting. Expectation values of the observables are estimated from averages over finite ensembles of matrices $\{\Phi\}$, characterised by a statistical weight which depends on the model dynamics; the algorithm generating the matrix ensemble is built combining overrelaxation steps [69, 70] and canonical updates.

For the configuration-updating process, different types of pseudo-random number generators were compared; the G05CAF generator of the NAG library has eventually been used in the production runs.

For each choice of the (N, r, λ, R) parameters, the autocorrelation time between elements in the thermalised matrix ensemble has been calculated using the auto-windowing procedure [71]; the expectation values of the various observables have been evaluated from ensembles of statistically uncorrelated matrices. The data analysis was done using standard techniques, and errorbars have been estimated using the jackknife method — see, for instance, [72].

Before presenting the numerical results in detail, it is instructive to discuss a few aspects intrinsic to the fuzzy space approach to a quantum theory, and their practical implications for the computer simulations; these aspects can be compared with the more conventional lattice field theory formulation:

- **The fuzzy space as a "dual" discretisation**
  The fuzzy space can be described as a "dual" discretisation, because it is based on quantisation of the algebra of functions on a given manifold. This is reflected in the implementation

of the Monte Carlo code, with dynamical variables associated to the degrees of freedom in the algebra, rather than to the value of the field at a given point.

- **Cut-off and symmetries**
  The lattice regularisation of a commutative field theory does not induce, *in se*, any non-commutativity. The physical results are obtained extrapolating the spacing a to zero, where the continuum space-time symmetries are restored, and — at least for the bosonic degrees of freedom[1] — the model exactly reproduces the features of the continuum theory. On the contrary, the spacetime symmetries are exactly preserved at every level in the fuzzy discretisation, but for every finite value of the N cut-off the fields are described by a non-commutative matrix algebra; a remnant of this non-commutative nature still survives the $N \to \infty$ limit, in the form of the non-commutative anomaly.

- **Loss of the notion of "points" and non-locality**
  In the fuzzy space formulation of a quantum theory, the notion of "points" in space no longer exists, although the effective cell-like resolution that one can achieve gets increasingly fine for larger and larger values of N. A related aspect is the intrinsic non-locality of the theory defined in a fuzzy space — a feature common to all non-commutative models.

- **Technical aspects of the numerical simulation**
  In lattice field theory there exist many efficient update methods (including, for instance, those described in [69, 70, 76–80]) which are based on the locality of the discretised action; these methods allow to strongly damp the autocorrelation among subsequent configurations in the Markov chain. Furthermore, parallel computation can often be implemented in a straightforward way. On the contrary, in the fuzzy setting, the dynamics of each degree of freedom is non-trivially entangled with each other's, and — in general — the implementation of analogous techniques is not trivial. However, it is clear that simulations of this model based on pure Metropolis updates do not achieve the best efficiency, and can be affected by severe thermalisation problems, as it was already noted in [58]. In the Appendix A, we shall discuss how an overrelaxation-like update technique improves the algorithm efficiency to explore the phase space of the model.

The use of a reliable simulation algorithm, which allows to explore the configuration space in an efficient way, is particularly important in the study of the structure of the "phase diagram"[2] of the model, as it will be discussed in subsection 3.1: for negative and large enough values of the r parameter, the typical matrix configurations are expected to lie in a neighbourhood of the minima of the potential:

$$\Phi = \pm\sqrt{-\frac{r}{2\lambda}}\mathbb{1} \ , \tag{10}$$

[1] The treatment of fermionic degrees of freedom on the lattice requires special care — see, for instance, [73–75] and references therein.

[2] Strictly speaking, phase transitions are expected only in the $R \to \infty$ limit; however, for finite values of R one can locate a susceptibility peak, and study its scaling properties as the model parameters are changed. This is the approach which was followed in [58, 59].

and a basic Metropolis algorithm would obviously face difficulties to mimic the tunneling events which connect the two regions.

3.1 Numerical results in the "broken symmetry" regime

In this subsection, we present the results obtained for the case when the symmetry of the classical potential is broken, *i.e.* when $r < 0$ in eq. (7).

In this regime, it is very interesting to study the behaviour associated with the various l-modes; in particular, the configurations in eq. (10) are associated to the classical minima of the potential: they correspond to uniform distributions and obviously their physical content is purely described by the scalar (l=0) channel. Since we are dealing with a quantum model and the system size is finite, the ground state is actually unique, as quantum fluctuations allow finite-action tunneling events between the two minima. When r is negative in sign and large in modulus, the profile of the potential is very steep, and the typical matrix configurations which one can expect typically lie in a close neighbourhood around the configurations in eq. (10); the trace of Φ is a clear detector (see figure 12 and figure 13) which allows to identify around which of the two minima the matrix is lying at a given Monte Carlo time. The "trace susceptibility", defined as:[3]

$$\chi = \langle (\mathrm{tr}\Phi)^2 \rangle - \langle |\mathrm{tr}\Phi| \rangle^2 \,, \tag{11}$$

encodes the physical information about the fluctuations of $\mathrm{tr}\Phi$. When r is increased to values closer to zero, the trace susceptibility exhibits a peak, corresponding to a maximum in the quantum fluctuations. As usual, the location of a maximum in the susceptibility approximately[4] identifies the critical value where the "phase transition" to the disordered phase would occur, for an infinite system.

Figures 1 to 5 show the results for the susceptibility obtained from runs with different matrix sizes; in particular, the diagrams correspond to values of λ which are scaled with N according to [59]. These plots display a sample of the results obtained from several different runs (information is summarised in table 1), which essentially reproduced the results obtained in [58, 59], with the increased precision allowed by our algorithm, and extending the analysis to include a larger number of λ and r values.

Next, we took a closer look at the matrix ensembles, and investigated their physical content in terms of the higher (*i.e.* non-zero) momenta, too. Our aim in doing so is to detect the presence of modes associated with non-uniform configurations on the sphere, and the rôle they play in the regime under consideration.

[3] Note the absolute value of $\mathrm{tr}\Phi$ appearing in the definition of χ: since the present system is finite (and no explicit symmetry-breaking term is included in the action), every non-zero expectation value for $\mathrm{tr}\Phi$ would actually be just a pure numerical artefact — and the conventional definition of χ would be a monotonically increasing function of $|r|$. The definition of χ in terms of the absolute value of the observable which would be a true order parameter for the corresponding infinite system is standard also for analogous problems in lattice field theory, and enables to highlight the physical information which is relevant to the limit one is usually interested in.

[4] Modulo finite-size corrections.

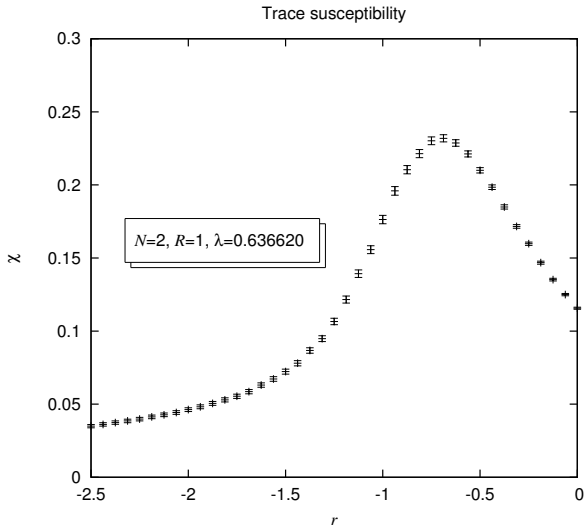

Figure 1: The trace susceptibility defined in eq. (11), plotted against r, for the parameters displayed.

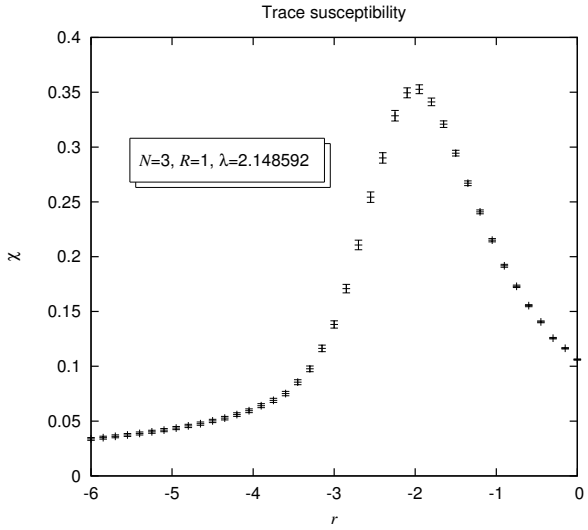

Figure 2: Same as in figure 1, but for different values of N and λ.

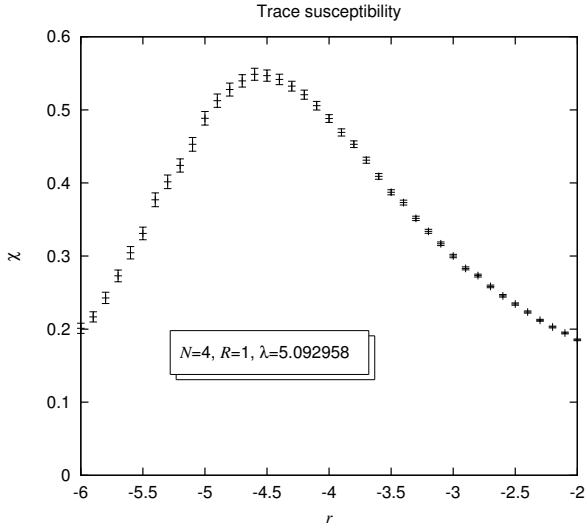

Figure 3: Same as in figure 1, but for different values of N and λ.

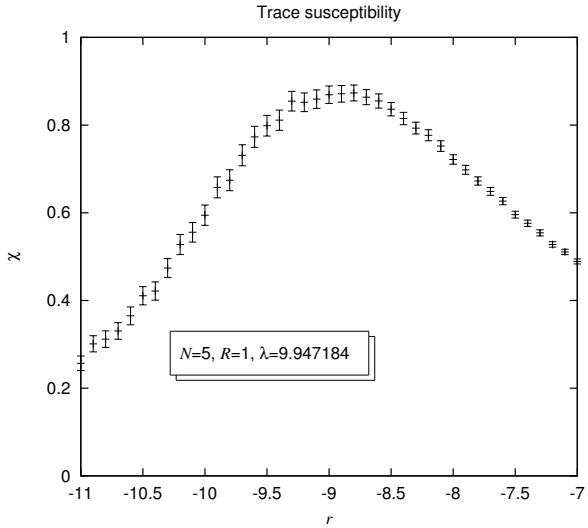

Figure 4: Same as in figure 1, but for different values of N and λ.

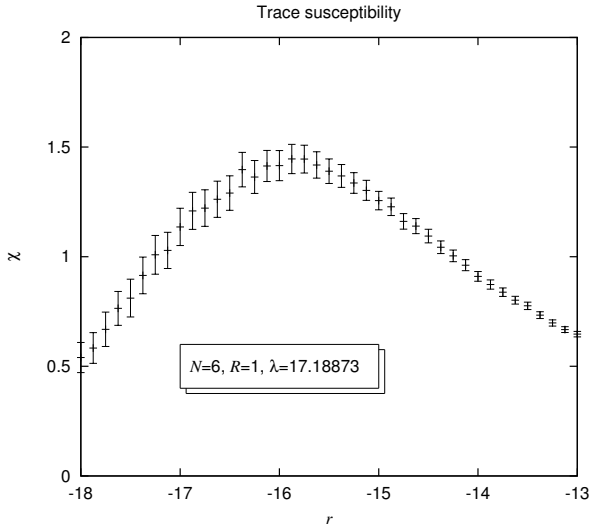

Figure 5: Same as in figure 1, but for different values of N and λ.

A simple variational analysis shows that also the commutative sphere can admit non-uniform configurations characterised by a finite, negative total amount of action.[5] Numerically, the relevance of these configurations can be detected — and measured — through the average values of the square moduli of the $c_{l,m}$ coefficients for $l \geq 1$.

As it can be expected from the theoretical arguments just outlined, the latter are indeed non-vanishing for all of the N, λ and r values investigated; again, in agreement with [58, 59], we found that there exist parameter ranges in which the expectation value of the $l = 1$ mode is larger than the scalar component.

However, we do not find solid arguments supporting the identification of the regime where the $l > 0$ modes have a non-negligible expectation value as a "non-uniform order phase" discussed in [58, 59], or the interpretation of the latter as an effect purely due to the non-commutativity induced by the fuzzy regularisation, or as a signature of a phenomenon analogous to UV/IR mixing.

Also, we have to say that our results appear not to be in complete agreement with the identification of the transition lines appearing in the phase diagram plotted in [59] — although the definition of the "transition lines" in this model is a subtle issue. This can be easily seen from the example that follows: we have investigated how the behaviour of various observables changes, along a line corresponding to $cN^{-2} = 1$ in figure 3 of [59];[6] according to that paper, a

[5] Although, for the purposes of the present paper, we did not concentrate on the analytical solution of the associated Euler differential equation, it is easy to see that — at least for certain values of the parameters — even an axially symmetric (but non-uniform) configuration parametrised in terms of first Legendre polynomial may be favoured with respect to the $\Phi = 0$ uniform configuration, and thus mediate the tunneling events among the classical minima of the potential.

[6] Note that the conventions in [59] differ with respect to [58] by an overall normalisation factor multiplying the

matrix size	n_λ	n_r	statistics
2	10	11, 31, 51, 101, 401	10 000, 200 000, 2 000 000
3	10	11, 31, 51, 101, 401	10 000, 200 000, 2 000 000
4	10	11, 31, 51, 201	10 000, 50 000, 100 000, 1 000 000
5	8	11, 16, 31, 201	10 000, 40 000, 80 000, 100 000, 500 000
6	8	11, 16, 31, 201	1 000, 20 000, 40 000, 100 000, 400 000
7	5	11, 16, 31, 201	1 000, 20 000, 40 000, 100 000, 400 000
8	5	11, 16, 31, 101	10 000, 20 000, 200 000
10	5	11, 16, 31, 101	10 000, 20 000, 100 000
12	3	11	1 000, 10 000, 20 000
15	1	8	1 000, 20 000

Table 1: Information about the statistics of the runs in the $r < 0$ regime; n_λ and n_r denote, respectively, the number of values of λ and of r at which the simulations were run. The number in the last column is the number of uncorrelated measurements which were taken, for each of the (λ, r) combinations (some of the lowest values actually include a preliminary binning over uncorrelated data). When several numbers appear, they refer to different values of the parameters in the previous columns.

"transition" between the "non-uniform order phase" and the "uniform order phase" should take place for $-bN^{-3/2} \simeq 5$, whereas another "transition", between the "disorder phase" and the "non-uniform order phase" should occur at approximately $-bN^{-3/2} \simeq 2$ (or slightly below), which is the third-order transition that one could predict from a "pure potential model" [67,68]. The data we obtained for exactly the same choice of parameters and normalisations do not confirm either of these results; this is manifest looking at figure 6 and figure 7 (where r corresponds to the b parameter in the notations of [59]): first of all, figure 6 — in which the expectation values of $|c_{0,0}|^2$ and of $\sum_{m=-1}^{1} |c_{1,m}|^2$ are plotted against $rN^{-3/2}$ — displays that, indeed, the component in the scalar channel dominates at large, negative values of r, while the $l = 1$ contribution is leading for smaller values of $|r|$. However, if one would like to identify the point where the "transition" between these two different regimes occurs, according to the definition of the "non-uniform order phase" given in [58], then one would say that this happens at approximately $rN^{-3/2} = -3.6$, rather than at the point predicted by the phase diagram in figure 3 of [59] (which is at about $rN^{-3/2} = -5$, and may be compatible with the location of the peak of the susceptibility plotted in figure 7).

Also, according to our data, it does not seem to be correct that a "phase transition" between the "non-uniform order" and the "disorder" regimes takes place at a value of $rN^{-3/2}$ near to -2 (or slightly closer to zero) — but in this case we should point out that the dashed line appearing in figure 3 of [59] is just an asymptotic prediction. Furthermore, we have to say that the whole interpretation of the transition from the "uniform order phase" to a "non-uniform order phase"

action; we have taken this into account.

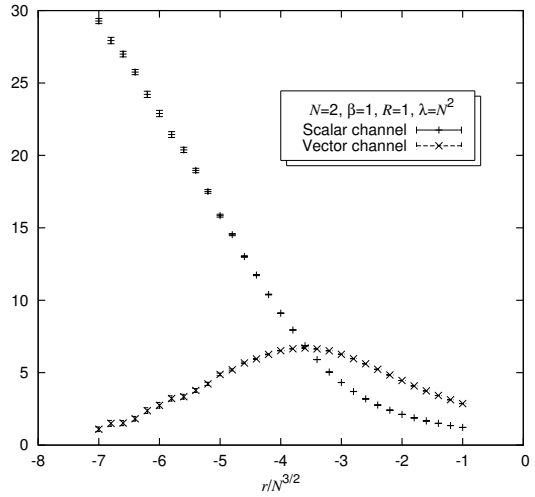

Figure 6: Expectation values of the square norm of the coefficients associated to the scalar and vector channels in the regime where the classical potential admits two degenerate minima, for the parameters displayed, which allow for a direct comparison with the results reported in [59].

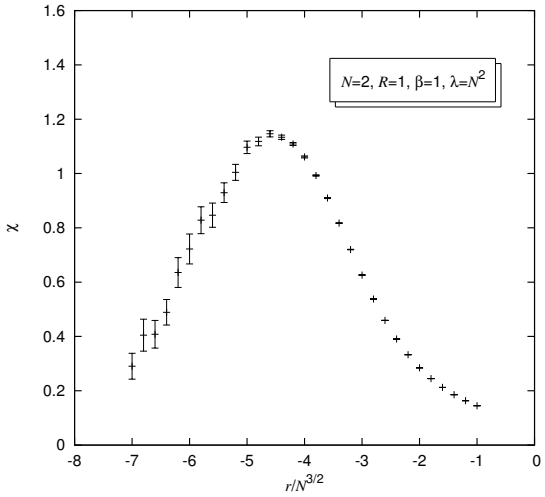

Figure 7: Behaviour of the trace susceptibility, as defined in eq. (11), for the same choice of parameters as in figure 6.

as an effect arising when the kinetic contribution to the action becomes negligible with respect to the potential one, as discussed in [58,59], appears not to be corroborated by our results. Figure 8 and figure 9 show, respectively, the average values of the kinetic and potential term contributions to the action, while the ratio of the former with respect to the absolute value of the latter is plotted in figure 10: the kinetic term dominates for values of r quite close to zero, and becomes comparable to the average contribution due to the potential for $rN^{-3/2} \simeq -1.4$, while it is smaller than the (modulus) of the average potential contribution for all of the data in the $rN^{-3/2} < -1.4$ range.

In particular, the precision of our results is such, that we can unambiguously state that the ratio of the kinetic contribution with respect to the potential one is monotonically increasing with r; this sets a serious problem for the interpretation of the "transition" between the "uniform order phase" and the "non-uniform order phase" which was presented in [58, 59]: in those papers, it was claimed that the "non-uniform order phase" arises when the kinetic term becomes negligible with respect to the potential one, as opposite to the (standard) "uniform order phase", in which the average kinetic term should be strong enough to remove the degeneracy of non-spherically-symmetric configurations. Our data show that exactly the opposite situation occurs: the contribution due to the potential becomes overwhelmingly dominating in the range of strongly negative values of r.

According to our results, it is indeed true that, in the (approximate) $-5 \lesssim rN^{-3/2} \lesssim -2$ range where — for $cN^{-2} = 1$ — the "non-uniform order" phase is expected to lie according to [59], the average kinetic contribution is smaller than the potential one; however, certainly

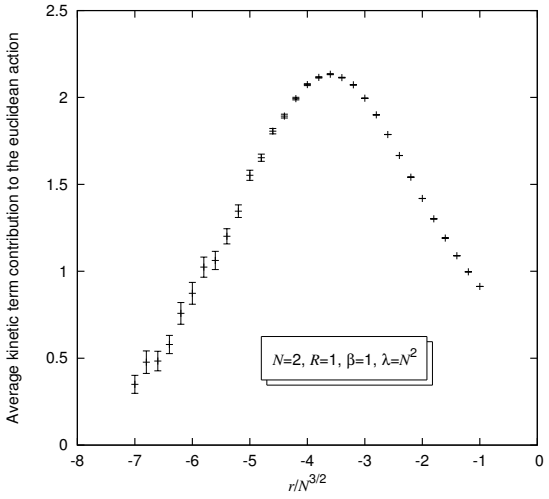

Figure 8: Average value of the kinetic energy contribution to the effective action; results are displayed for the same choice of parameters as in figure 6.

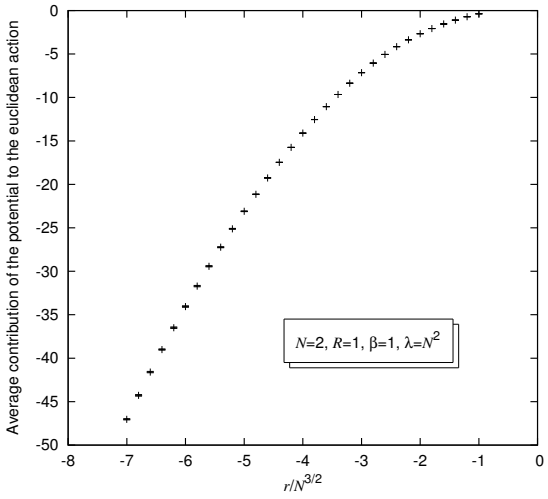

Figure 9: Average value of the potential contribution to the effective action, for the same choice of parameters as in figure 8.

one cannot claim that for $rN^{-3/2} \lesssim -5$ the kinetic term becomes relevant again, so to shift the degeneracy associated to non-spherically-symmetric configurations. Therefore, according to our data, the interpretation of the "non-uniform order phase" (or, better: of the presence of non-spherically-symmetric configurations) purely in terms of a pure potential model appears to be at least questionable, since it does not explain why the "uniform order phase" would eventually set in.

In the opposite limit, we cannot confirm the assumption that the relative weight of the kinetic term contribution to the action is numerically negligible even for values $rN^{-3/2} \simeq -2$, or larger (which corresponds to the dashed line plotted in figure 3 of [59]), because in that case our data show that the kinetic term is still as large as about 50% with respect to the (absolute value of the) potential.

If the interpretation of the data in terms of the pure potential model discussed in [67, 68] were based on the assumption that the kinetic term contribution to the action is negligible in the "non-uniform order phase" [58, 59], then we could not confirm this scenario; however, as we remarked above, the prediction of the pure potential model is an asymptotic one, and significant deviations can show up for finite values of N. In any case, our results are compatible with the fact that, in a certain parameter range, the tunneling between the minima of the potential may be mediated by matrix configurations which correspond to non-spherically-symmetric distributions on the sphere. For this quantum system, this can be easily justified from the analytical point of view (evaluating explicitly the action associated to such configurations), and appears to be fully consistent with the numerical results (which confirm a non-negligible expectation value for the modes with $l \neq 0$ when r is not very far from zero).

Finally, we remark that in principle this interpretation is fully consistent both for the fuzzy sphere setting and for the commutative sphere setting. On the other hand, in subsection 3.2

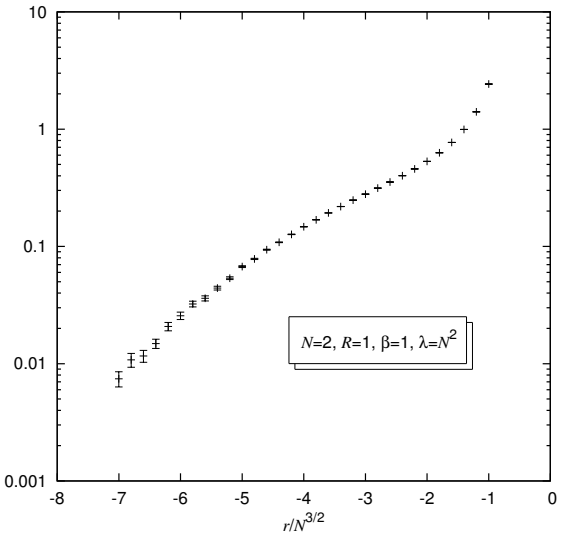

Figure 10: The ratio between the average kinetic contribution and the modulus of the average potential contribution for the same parameters as in previous figures. Note that the results are plotted using a logarithmic scale for the vertical axis.

we shall address a numerical study of an effect purely due to the non-commutativity anomaly intrinsic to the fuzzy sphere.

3.2 Numerical results in the "unbroken symmetry" regime

In this subsection, we present the results obtained for the case when the classical potential has a unique minimum.

A perturbative study of the model in this regime was presented in [49]; we redefine the action of the matrix model as:

$$S = \frac{4\pi}{N+1}\mathrm{tr}\left(\frac{1}{2}\left[L_i,\Phi\right]^\dagger\left[L_i,\Phi\right] + \frac{\mu^2}{2}\Phi^2 + \frac{g}{4!}\Phi^4\right) \tag{12}$$

in order to make contact with the conventional notations, which are also used in [49]; here the size of the hermitian matrix Φ is denoted as $N+1$.

We focus on the non-commutative anomaly: our aim is to look for a signature of this effect in the numerical results. As it was discussed above, the non-commutative anomaly shows up as a (mild) non-local effect, distorting the energy-momentum relation on the fuzzy sphere by a finite amount.

The importance of this effect is twofold: on one hand, this anomaly implies that the naïve formulation of a scalar model on the fuzzy sphere cannot be considered as a valid regularisation scheme reproducing the full features of the scalar QFT in commutative space, when the $N \to \infty$

limit is taken.[7] On the other hand, the non-commutative anomaly is responsible for the rise of the UV/IR mixing phenomenon on the non-commutative plane, which can be obtained in a scaling limit when the radius of the sphere R and the matrix size N are sent to infinity in such a way, that the $\frac{R^2}{N}$ ratio is held fixed. In this limit, the non-commutative anomaly induces a divergence in the one-particle-irreducible two-point function.

The perturbative study presented in [49] showed that the one-loop effective action on the fuzzy sphere is:

$$S_{\text{one-loop}} = S_0 + \frac{4\pi}{N+1}\text{tr}\left[\frac{\delta\mu^2}{2}\Phi^2 - \frac{g}{24\pi}\Phi h\left(\tilde{\Delta}\right)\Phi\right] + O\left(\frac{1}{N}\right) \ , \tag{13}$$

where $\delta\mu^2$ is the square-mass renormalisation:

$$\delta\mu^2 = \frac{g}{8\pi}\sum_{J=0}^{N}\frac{2J+1}{J(J+1)+\mu^2} \ , \tag{14}$$

while the non-commutative anomaly is given by the contribution involving $h\left(\tilde{\Delta}\right)$; $h(x)$ is the harmonic number: $h(x) = \sum_{t=1}^{x}\frac{1}{t}$, with $h(0) = 0$, and $\tilde{\Delta}$ is a function of the Laplace operator, whose eigenvalue when acting on $\hat{Y}_{l,m}$ is l.

In order to test numerically this prediction, the parameters of the model have to be tuned in such a way that the hypotheses underlying the derivation of eq. (13) are satisfied. In particular, g and $\frac{1}{N}$ must be sufficiently small, so that higher order contributions are indeed negligible.

From the practical point of view, it is not easy to disentangle among the various terms contributing to the effective action; in particular, $S_{\text{one-loop}}$ contains three terms of order g: the quartic interaction term in S_0, the square mass renormalisation term, and the non-commutative anomaly term. Observe that the quartic interaction term can be neglected, if $\text{tr}\Phi^4$ is always much smaller than $\text{tr}\Phi^2$ in the typical configurations contributing to the quantum ensemble; this can be achieved by choosing the model parameters appropriately. Then the residual dependence on g can be studied more easily, by virtue of the fact that the square-mass renormalisation is a momentum-independent effect, whereas the non-commutative anomaly distorts the dispersion relation.

Therefore, a possible way to check the non-commutative anomaly effects in the numerical results consists in studying the distortion of the spectrum of relative weights associated with the various spin channels, as g is changed; in a parameter range where the various assumptions hold (at least approximately), and in which the numerical precision is sufficient to detect these fine effects, one expects to observe larger probabilities for higher l channels, when g is increased.

We should point out that the concurrent restrictions imposed by the analytical approximations and by practical limitations severely reduce the window of data where a signal may be observed and compared with the theoretical prediction in a reliable way. In order to reach a range of

[7] As it was discussed in [65], a possible way to avoid this problem would be to define the interaction term via a normal-ordering prescription. An alternative (and more general) possibility [66] may be to define an "improved" version of the original action, including a higher-derivative term with a tunable parameter.

parameters where we could obtain precise enough results, we first addressed a preliminary study, investigating moderate matrix sizes, and tried to push our analysis down to the smallest values of N, where the highest statistics could be obtained.

Going to too small N-values may induce significant deviations with respect to the asymptotic formulæ in [49]. Still, the impact of these deviations can be quantified; for instance, the following asymptotic expression for the $6j$-symbols [81, 82]:

$$\left\{ \begin{array}{ccc} k & k & l \\ k & k & j \end{array} \right\} \simeq \frac{(-1)^{l+j+2k}}{2k} P_l \left(1 - \frac{j^2}{2k^2} \right) \tag{15}$$

(where $P_l(x)$ is the Legendre polynomial of order l) is only expected to hold when $l \ll k$ and k is large. However, even for some value ranges which do not satisfy these constraints, the deviations are relatively small; we have carefully checked that the systematic error induced by the approximations (where they were used) on the final (net) observed signal was never larger than $O(10^{-1})$. In fact, one may expect that a signature of the asymptotic behaviour is still present in the numerical data, even for borderline values of the parameters.

The data analysis confirms that the approximations are under control. Also, table 2 shows, for instance, that, when g is varied, the zero-channel mode appears not to be affected by anomalous contributions: this is consistent with the fact that, for $l = 0$, the contributions from a non-planar diagram and from a planar one are equal — an exact result, which does not depend on any approximation.

Encouraged by these observations, we have then addressed a study of the higher channels, focusing on how $\Pi_l(g)$, the power[8] of the modes associated to intermediate l values, varies with g.

The results give an indication that $\Pi_l(g)$ is (slowly) increasing with g, in agreement with the theoretical prediction. In particular, figure 11 shows an example of comparison between the results for the power in one of the intermediate channels, and an approximate prediction (which would be exact in the limit of "monochromatic" matrices), consistent with the average value of the trace of Φ^2 in the sample. This prediction is only meant to give a rough estimate of the order of magnitude which can be expected for the shift induced by the non-commutative anomaly, but the agreement, especially for these data obtained from a high-statistics sample of matrices, appears to be quite remarkable.

In general, all data sets for which a sufficient precision was reached show that fitting the results of the $l > 0$ channels to functions like the one plotted in figure 11 yields better values for the reduced χ^2 than assuming no non-commutative anomaly, as table 3 shows.

The statistics accumulated for large matrices did not allow to get more precise results; however, data analysis shows again that, for all of the sets where a signal was clearly observed, its sign agrees with the expected shift, and its order of magnitude is roughly comparable with the prediction, even in the less-favourable cases.

Table 3 shows information about the data analysis, giving some quantitative support to these claims. The results obtained from the data sets where the best precision was obtained appear

[8]Here and in the following, we refer to the average square modulus of the coefficients associated with a given angular momentum l as to the "power" in that channel.

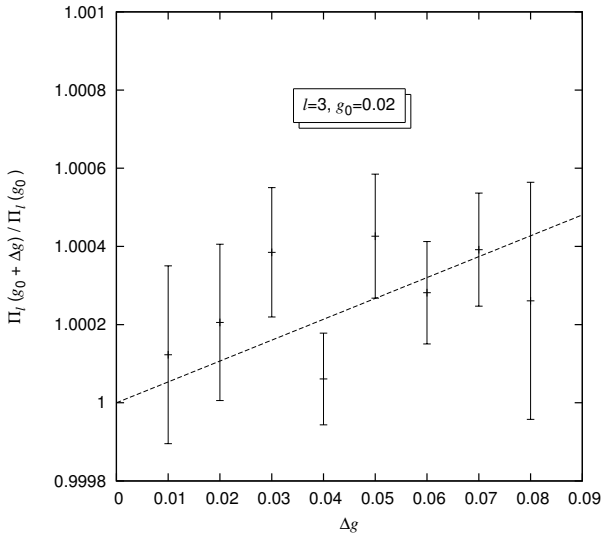

Figure 11: The non-commutative anomaly tends to favour the channels associated to non-vanishing momenta. The figure shows the results, for a given channel, obtained from a matrix sample with $N + 1 = 7$, $\mu^2 = 200$, in comparison with the theoretical prediction (dashed line) discussed in the text.

to be consistent with the predicted non-commutative anomaly (although it is not possible to unambiguously establish whether the signal observed is purely due to the latter, or to a possible combination of effects including other contributions, too). On the other hand, our results do not allow to formulate a conclusive statement for the larger matrices, due to the lower precision of the data; in that case, however, the results do not contradict the expectation either, and no other spurious effects are observed.

Therefore, we can conclude that — at least in the limited range in which we concentrated our computational efforts to reach high enough precisions — our algorithm has allowed to observe the signature of a fine but highly non-trivial effect, which is intrinsically related to non-locality, and which is due to the anomalous contribution that shows up, when the fuzzy sphere is used as a regulator for a scalar model.

4 Discussion

The data in the previous section confirm the theoretical predictions for a scalar theory on the fuzzy sphere, as well as previous numerical results for the same model. The novel algorithm we used for the simulation proved to be very efficient, enabling us to obtain high-precision results for both the regimes that were investigated — namely, for a potential with unbroken or with spontaneously broken symmetry — within a limited amount of computational time.

As it concerns the case of a classical scalar potential with two degenerate minima, we have

investigated a large number of points in the space of physical parameters of the model, and essentially confirmed the results obtained in similar numerical works [58, 59]. In particular, we have observed the behaviour of physical modes corresponding to different momenta, which fits in the general picture expected for this quantum system: tunneling events connect the classical vacua, and this effect can be mediated by configurations which are not spherically symmetric. The latter are characterised by a finite amount of euclidean action on the finite radius sphere, and — depending on the parameter values — may be favoured with respect to other spherically symmetric configurations. We would like to emphasise that this phenomenon is not due to the non-commutative nature of the fuzzy regularisation, nor can it be directly interpreted as a signature of any kind of UV/IR mixing (UV/IR mixing, indeed, *does not* take place on the fuzzy sphere). It may be instructive to point out that the situation here is completely different with respect to the case of an infinite plane, where a global configuration change from the neighbourhood of one minimum to the other is possible when the correlation length diverges — in that case, a phase transition occurs.

On the other hand, the non-commutative deformation of these spaces introduces further effects: a finite non-commutative anomaly appears on the fuzzy sphere with finite radius, whereas the UV/IR mixing phenomenon and the new, striped phase show up on the non-commutative plane. A particularly interesting and crucially important aspect is that the non-commutative anomaly induces the logarithmic infrared divergence characteristic of the UV/IR mixing, once the double-scaling limit for R and N is taken, to recover the non-commutative plane.

The latter issue is indeed one of the most intriguing features of the fuzzy sphere approach: it allows to interpret the UV/IR mixing effect as the singular limit of a finite, non-local, non-commutative anomaly.

The importance of this effect led us to address a numerical study of the non-commutative anomaly, in the region where the classical potential has a unique minimum. A well-suited tuning of the parameters allows to access the regime where the full non-perturbative numerical analysis can match the perturbative predictions; we combined this with a precise choice of the observables of interest, in order to focus our attention onto the modification of the dispersion relation which is induced by the anomalous, non-local term. The precision of our results allowed us to observe the expected behaviour, although the range of data which could be used to make a meaningful comparison was severely limited by the various constraints on which the analytical predictions rely, as well as by the need to reach sufficient numerical precision.

Therefore, according to our results, the theoretical expectations for this model in the two different regimes are confirmed, and our algorithm appears to be an efficient tool for this kind of studies. Its performances, which have been thoroughly tested before the production runs (as reported in the Appendix A), are confirmed by the good precision obtained for the final results.

5 Summary and conclusions

In summary, in this paper we have presented a precise numerical study of a scalar theory defined on a non-commutative space: we have addressed the problem through Monte Carlo simulation

of the model regularised on the fuzzy sphere, devising an update procedure inspired by the overrelaxation algorithm which is commonly used in lattice gauge theory. We have tested this algorithm and studied its performance, showing that it allows one to explore efficiently the phase space of the model. The key-point underlying its efficiency is related to the fact that it strongly reduces the correlation among subsequent configurations in a Markov chain, in a way which is compatible with the dynamics of the quantum system, and limiting any undesired numerical artefacts to a minimum.

Then we have used this algorithm to investigate the physical content of the quantum scalar model on the fuzzy sphere: for a potential with quartic interactions, we have studied both the case when the classical vacuum is doubly-degenerate, and the unbroken-symmetry case.

In the first case, we have studied the trace susceptibility and the distribution of modes associated with different momenta, in comparison with the numerical results obtained in some previous studies of the same model. We have pointed out a new interpretation of these data, remarking the relevance of tunneling events mediated by non-spherically-symmetric configurations with finite action, which make the true quantum vacuum unique, and we have clarified the rôle of the $l > 0$ modes in the numerical results.

On the other hand, in the regime where the classical ground state of the potential is non-degenerate, we have studied the quantum effective action, investigating the contribution given by the non-commutative anomaly which is induced by the regularisation of the theory on the fuzzy sphere; we remarked on the theoretical implications of this anomaly, and its impact on the fuzzy approach as a regularisation program for QFT, mentioning some proposals which have been suggested in order to avoid this problem. Then we have penetrated the perturbative domain of the theory with our non-perturbative tool, exploring a parameter range where the numerical results are expected to match the one-loop analytical predictions, and we have observed a signal for the non-local distortion of the dispersion relation induced by the non-commutative anomaly. We have commented on and taken care of the various approximations involved, and found evidence for the effects predicted theoretically.

In conclusion, we can say that the non-perturbative results obtained in the present work confirm the current theoretical understanding of this simple non-commutative model, and the virtues and limits of the fuzzy approach as a candidate regularisation method for QFT. As it is clear that a non-commutative anomaly does exist, and that its rôle cannot be neglected, it would be interesting to study in detail the proposals which have been formulated [65, 66] to possibly define an improved formulation of the action, yielding the correct QFT limit.

Another possible generalisation to pursue would be the inclusion of some kind of supersymmetry in the fuzzy setting, as one may hope that it cancels the non-commutative anomaly. So far, supersymmetric theories on the fuzzy sphere have been proposed [83–85], but a full-fledged interacting theory has not been obtained yet.

On the other hand, a further line of research on fuzzy manifolds arises when they are considered as a regularisation for intrinsically non-commutative spaces, like, for instance, those which are relevant to solid-state physics problems, or to string theory; also in this cases, efficient Monte Carlo simulations can offer a useful non-perturbative insight into the dynamics of models which are of the utmost importance for our understanding of Nature.

Acknowledgements.
The author thanks the international community of scientists working on fuzzy physics for enlightening discussions, as well as M. Caselle, M. Hasenbusch and W. Nahm for helpful comments on some aspects discussed in this work, and acknowledges support received from Enterprise Ireland under the Basic Research Programme.

A An overrelaxation algorithm for the fuzzy sphere

In order to investigate the structure of the "phase diagram" of the model, it is desirable to use an algorithm which allows to explore the phase space in an efficient way. In [58], where a self-adaptive version of the Metropolis algorithm was used, it was pointed out that the numerical observation of the phase transitions was difficult, because of autocorrelation problems, and numerical artefacts — including a dependence on the initial conditions of the matrix — could heavily affect the results; the analysis, however, was later extended to larger statistics [59]. In order to overcome these problems without resorting to a brute force approach, a slightly more sophisticated algorithm is required.

Here, we describe a novel algorithm, that improves the efficiency of the Monte Carlo integration for the model considered, by damping the autocorrelation between subsequent elements in the chain of configurations.

The basic idea is closely related to the overrelaxation technique in lattice gauge theory [69,70], which, in turn, is inspired by the overrelaxation algorithms used for the numerical solution of difference equations: the trial value in the update process of a given variable is chosen to be "as far as possible" from the original value. For lattice gauge theory, the trial value is chosen through a group reflection of the original matrix, which preserves the value of the action;[9] this can be worked out exactly for the $SU(2)$ group, and in an efficient way for a generic $SU(N)$ group [86,87]. This technique cannot be directly implemented in the present case, due to the fact that the Φ variable takes values in a domain of different nature: the space of hermitian matrices of size N is non-compact, and, more important, a naïve "reflection" of the Φ matrix would not be effective for the purpose of reducing the autocorrelation time, since it would not allow to explore all of the physical orbits.

Therefore, we have built an algorithm which generalises the principia underlying the overrelaxation technique, adapting them to the present case.[10] This algorithm has been used in combination with a sequence of standard ergodic updates; its implementation, as described below, depends on one free parameter, which has been tuned according to optimisation criteria. The algorithm has been tested for a large number of combinations of the (λ, r, N) parameters, belonging to different physical regimes, and the results have been compared with those obtained from configuration ensembles produced using a conventional Metropolis procedure: the expectation values are consistent for all of the observables, whereas the precision is improved, by virtue of the fact that all correlation effects are strongly damped by the overrelaxation steps in the new algorithm.

The algorithm works as follows: assume Φ_0 to be the initial matrix configuration, obtained with some ergodic procedure; let $S_0 = S(\Phi_0)$ be the associated euclidean action. Let $\Phi_\star$ be a new, completely random (and, therefore, completely independent from Φ_0) hermitian matrix in Mat_N, with $S_\star = S(\Phi_\star)$ the corresponding value of the action. If $S_\star > S_0$,[11] then it is elementary

[9] This implies that the overrelaxation procedure is microcanonical; therefore the method is always combined with other canonical techniques, in order to ensure ergodicity of the whole update process.

[10] Henceforth, we shall refer to it as to the "overrelaxation algorithm".

[11] If $S_\star \leq S_0$, then $\Phi_\star$ is accepted as the new matrix configuration.

to prove that a new hermitian matrix Φ_1, such that: $S_1 = S(\Phi_1) = S_0$, can be built rescaling $\Phi_\star$ as:

$$\Phi_1 = \alpha \Phi_\star, \tag{A.1}$$

provided the following condition:

$$\left\{ (S_0 > 0) \ \vee \ \left(\mathrm{tr}\left(\Phi_\star^4\right) > \frac{N S_\star}{4\pi\lambda} \right) \right\} \tag{A.2}$$

is true. If that is not the case, then $\Phi_\star$ is redefined (possibly iteratively) as:

$$\Phi_\star \longrightarrow \frac{\Phi_\star + \Phi_0}{2} \tag{A.3}$$

until the condition in eq. (A.2) is satisfied. Note that this shift would drive $\Phi_\star$ closer and closer to Φ_0, thus inducing a correlation between corresponding matrix entries in Φ_1 and Φ_0; nevertheless, in general the eventual value obtained for Φ_1 may belong to a different physical orbit with respect to Φ_0.

The algorithm is efficient under general conditions, including the cases in which $S(\Phi)$ is a function which varies strongly even for moderate changes in its argument, because the process driving $\Phi_\star$ towards Φ_0 is exponentially fast, its implementation only involves trivial numerical operations, and terminates in a finite (and typically small) number of steps.[12]

The algorithm allows the freedom to choose the starting value for the hermitian matrix $\Phi_\star$ according to an arbitrary distribution; in order to achieve the best efficiency, various possibilities were tested, and in the production runs we eventually chose the matrix elements of $\Phi_\star$ according to a gaussian distribution centered around zero; the width of the gaussian was tuned according to an optimisation criterion.

Table 4 displays information about the algorithm efficiency ξ, for some choices of the parameters.[13] On the other hand, table 5 shows information about the behaviour of the acceptance rate in the update process, for some of the typical parameters that were considered.

In order to study how effective our algorithm is in exploring the phase space, we focused on two different observables of interest, considering the Monte Carlo evolution of the trace of the matrix, and the average self-correlation of the matrix degrees of freedom.

The Monte Carlo history of $\mathrm{tr}(\Phi)$ in the regime where the classical scalar model would admit two distinct, degenerate vacua gives a clear indication of the fact that our algorithm explores the phase space of the full quantum system in an efficient way, sampling configurations around different minima; figure 12 shows an example of Monte Carlo history — in which only decorrelated measurements are displayed — of the matrix trace (which is proportional to the $c_{0,0}$ physical component), obtained without overrelaxation: in the set of data shown, only two tunneling events occur. On the other hand, figure 13 presents the analogous evolution, obtained with our

[12] This is easily proven using continuity and the fact that the trivial $\alpha = 1$ solution exists for $\Phi_\star = \Phi_0$.

[13] We have to say that it is difficult to quantify precisely the gain in ξ obtained with our algorithm, because the efficiency of the Metropolis algorithm can vary very much, depending on the size of the interval for the proposed updates of the variables.

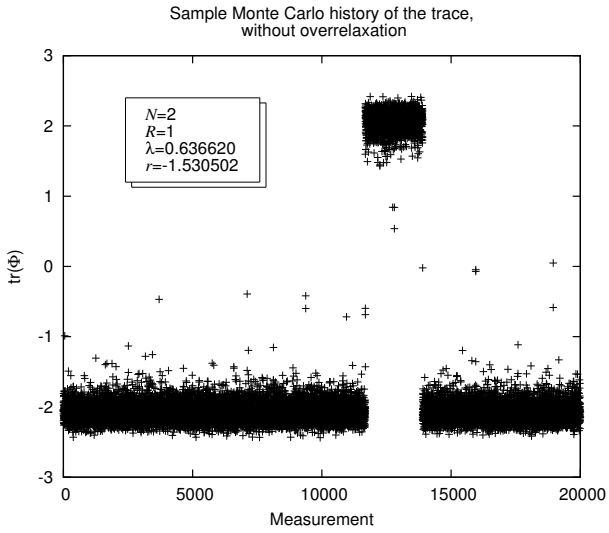

Figure 12: A typical Monte Carlo history of $\mathrm{tr}(\Phi)$ in the $r < 0$ regime, obtained without overrelaxation; the data fluctuate close to one of the two minima of the potential, and tunneling events are very rare.

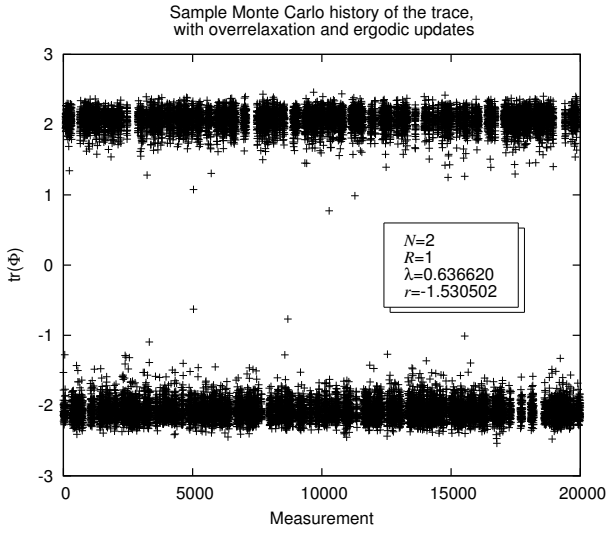

Figure 13: Same as in fig. 12, but for data obtained with our algorithm; the overrelaxation steps enhance the possibility of tunneling events with respect to the previous case.

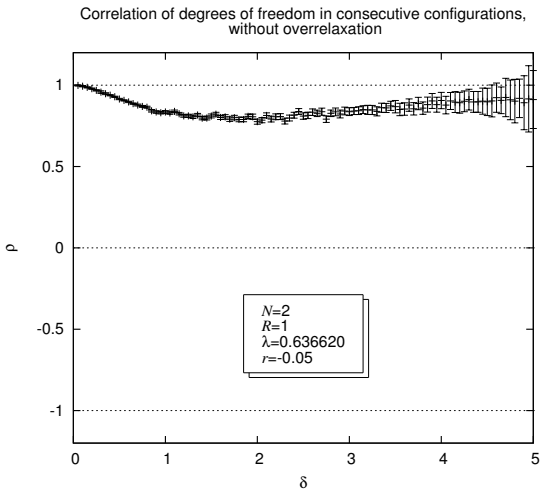

Figure 14: Average self-correlation for the degrees of freedom of consecutive matrices in a Markov chain obtained without using the overrelaxation procedure. Data are plotted against δ, the width of the uniform distribution for the proposed variations in the entry-by-entry update process.

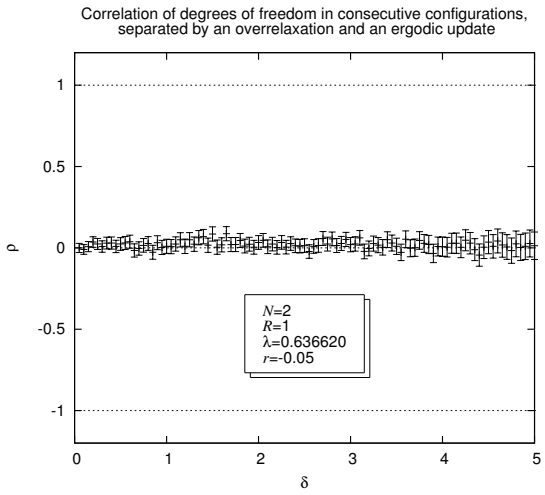

Figure 15: Same as in figure 14, but for matrices in a Monte Carlo ensemble obtained combining overrelaxation and ergodic updates. In this case, the degrees of freedom are almost completely uncorrelated.

algorithm: in this case, the number of tunneling events is of order thousands — comparable with the total number of measurements taken. This feature holds for a generic choice of the parameters: in particular, the ratio expressing the gain in CPU-time required for the same accuracy is an increasing function of the matrix size N. The Monte Carlo evolution induced by our algorithm is highly efficient because the overrelaxation steps allow for large changes in the matrix entries, in a way which is consistent with the system dynamics.

In particular, the correlation among the degrees of freedom in consecutive matrices in the Monte Carlo history is efficiently damped (down to values very close to zero,[14] as it is expected); as an example, figure 14 shows the average auto-correlation for the various degrees of freedom after a single Metropolis update, and its dependence on the width δ of the distribution for the proposed variations of the matrix entries, for a given choice of parameters. On the other hand, figure 15 shows the radically different behaviour of the same quantity, when the overrelaxation routine is combined with an ergodic update, under the same conditions.

It is also interesting to study the efficiency of the algorithm as a function of the distribution which is used to generate the (pseudo-)random entries of the proposed $\Phi_\star$ matrix; our experience gave us insight that — in general — a gaussian distribution proves to be (slightly) more efficient in comparison to a compact-support distribution characterized by the same variance σ^2; a comparison between the efficiency obtained using a gaussian *versus* a uniform distribution is summarised in table 6. Therefore, we decided to use a symmetric gaussian distribution for the

[14] A small and positive residual correlation is observed, which may be interpreted as an effect induced by those cases when the new matrix is shifted before being rescaled.

production runs; with this choice, the algorithm performances were studied, as a function of the distribution width. As an example, we display two plots obtained studying the cases when the $\Phi_\star$ matrix is shifted towards Φ_0; the latter may play a key rôle to the algorithm efficiency, as they are responsible for inducing correlation between Φ_0 and Φ_1: therefore, it is important to tune the distribution in such a way, that the number of their occurrences is under control. The data shown here correspond to a particular choice of parameters, but the results obtained for different sets of parameters led to the same qualitative conclusions; figure 16 shows the average number of

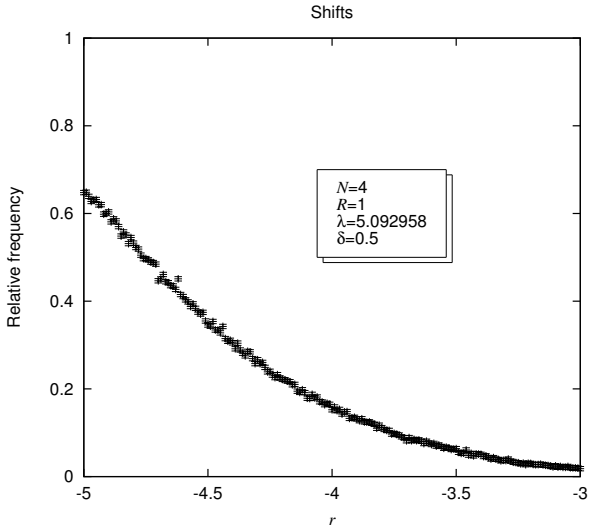

Figure 16: A plot of the relative frequency of occurrences of cases in which the matrix shift is invoked, for the choice of parameters displayed.

cases when shifts are required, while figure 17 shows the average number of shifts implemented to obtain convergence, in those cases when shifts are required, plotted against the distribution width σ; note that the figure suggests a dependence on σ weaker than a linear one.

Keeping into account that the eventual average auto-correlation is nevertheless very small, the combination of rescaling and shifts underlying the construction of the algorithm appears to be expedient and highly effective; furthermore, it is interesting to note that the relative frequency of cases in which the generated matrix yields a lower value of the action in general is not negligible — see, for instance, figure 18. This piece of information, combined with the observation of the high rate of tunneling events, leads us to the conclusion that the algorithm is highly effective in spanning all the statistically relevant regions in the phase space.

References

[1] S. Doplicher, K. Fredenhagen and J. E. Roberts, Commun. Math. Phys. **172** (1995) 187 [arXiv:hep-th/0303037].

Figure 17: The number of iterations implemented to obtain convergence, averaged over the population of cases when shifts are required, for the choice of parameters displayed.

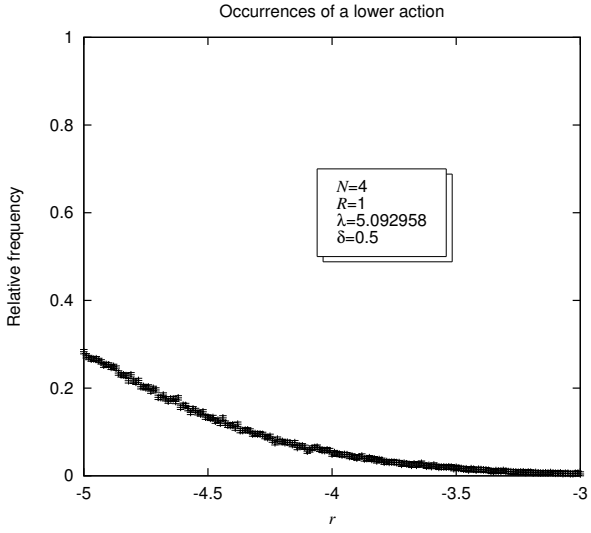

Figure 18: Frequency of new matrix configurations characterised by lower values of the action, for the choice of parameters displayed.

[2] G. Landi, arXiv:hep-th/9701078.

[3] M. R. Douglas and N. A. Nekrasov, Rev. Mod. Phys. **73**, 977 (2001) [arXiv:hep-th/0106048].

[4] R. J. Szabo, arXiv:hep-th/0606233.

[5] W. Pauli, "Scientific Correspondence," Vol. II, (Ed. Karl von Meyenn, Springer-Verlag, 1985), p. 15.

[6] W. Pauli, "Scientific Correspondence," Vol. III, (Ed. Karl von Meyenn, Springer-Verlag, 1993), p. 380.

[7] H. S. Snyder, Phys. Rev. **71** (1947) 38.

[8] C. N. Yang, Phys. Rev. **72** (1947) 874.

[9] J. E. Moyal, Proc. Cambridge Phil. Soc. **45** (1949) 99.

[10] D. Karabali, V. P. Nair and S. Randjbar-Daemi, arXiv:hep-th/0407007.

[11] A. Connes, M. R. Douglas and A. S. Schwarz, JHEP **9802**, 003 (1998) [arXiv:hep-th/9711162].

[12] M. R. Douglas and C. M. Hull, JHEP **9802**, 008 (1998) [arXiv:hep-th/9711165].

[13] A. Y. Alekseev, A. Recknagel and V. Schomerus, JHEP **9909** (1999) 023 [arXiv:hep-th/9908040].

[14] N. Seiberg and E. Witten, JHEP **9909** (1999) 032 [arXiv:hep-th/9908142].

[15] A. H. Chamseddine, G. Felder and J. Fröhlich, Commun. Math. Phys. **155** (1993) 205 [arXiv:hep-th/9209044].

[16] S. Doplicher, K. Fredenhagen and J. E. Roberts, Phys. Lett. B **331** (1994) 39.

[17] S. Doplicher, arXiv:hep-th/0105251.

[18] T. Filk, Phys. Lett. B **376**, 53 (1996).

[19] G. H. Chen and Y. S. Wu, arXiv:hep-th/0103020.

[20] A. Jain and S. D. Joglekar, Int. J. Mod. Phys. A **19**, 3409 (2004) [arXiv:hep-th/0307208].

[21] M. Chaichian, P. P. Kulish, K. Nishijima and A. Tureanu, Phys. Lett. B **604**, 98 (2004) [arXiv:hep-th/0408069].

[22] R. J. Szabo, Phys. Rept. **378**, 207 (2003) [arXiv:hep-th/0109162].

[23] S. Minwalla, M. Van Raamsdonk and N. Seiberg, JHEP **0002**, 020 (2000) [arXiv:hep-th/9912072].

[24] I. Hinchliffe, N. Kersting and Y. L. Ma, Int. J. Mod. Phys. A **19**, 179 (2004) [arXiv:hep-ph/0205040].

[25] S. S. Gubser and S. L. Sondhi, Nucl. Phys. B **605**, 395 (2001) [arXiv:hep-th/0006119].

[26] E. Langmann and R. J. Szabo, Phys. Lett. B **533** (2002) 168 [arXiv:hep-th/0202039].

[27] H. Grosse and R. Wulkenhaar, Commun. Math. Phys. **256** (2005) 305 [arXiv:hep-th/0401128].

[28] V. Rivasseau, F. Vignes-Tourneret and R. Wulkenhaar, Commun. Math. Phys. **262** (2006) 565 [arXiv:hep-th/0501036].

[29] T. R. Govindarajan, S. Kürkçüoğlu and M. Panero, Mod. Phys. Lett. A **21** (2006) 1851 [arXiv:hep-th/0604061].

[30] H. Grosse and H. Steinacker, Nucl. Phys. B **746** (2006) 202 [arXiv:hep-th/0512203].

[31] H. Grosse and H. Steinacker, arXiv:hep-th/0603052.

[32] H. Grosse and H. Steinacker, arXiv:hep-th/0607235.

[33] J. Ambjørn, Y. M. Makeenko, J. Nishimura and R. J. Szabo, Phys. Lett. B **480** (2000) 399 [arXiv:hep-th/0002158].

[34] J. Ambjørn, Y. M. Makeenko, J. Nishimura and R. J. Szabo, JHEP **0005** (2000) 023 [arXiv:hep-th/0004147].

[35] T. Azuma, S. Bal, K. Nagao and J. Nishimura, JHEP **0405**, 005 (2004) [arXiv:hep-th/0401038].

[36] W. Bietenholz, F. Hofheinz and J. Nishimura, JHEP **0209** (2002) 009 [arXiv:hep-th/0203151].

[37] W. Bietenholz, F. Hofheinz and J. Nishimura, Nucl. Phys. Proc. Suppl. **119** (2003) 941 [arXiv:hep-lat/0209021].

[38] J. Ambjørn and S. Catterall, Phys. Lett. B **549**, 253 (2002) [arXiv:hep-lat/0209106].

[39] W. Bietenholz, F. Hofheinz and J. Nishimura, JHEP **0406** (2004) 042 [arXiv:hep-th/0404020].

[40] W. Bietenholz, A. Bigarini, F. Hofheinz, J. Nishimura, Y. Susaki and J. Volkholz, Fortsch. Phys. **53** (2005) 418 [arXiv:hep-th/0501147].

[41] W. Bietenholz, J. Nishimura, Y. Susaki and J. Volkholz, arXiv:hep-th/0608072.

[42] J. Madore, Class. Quant. Grav. **9** (1992) 69.

[43] G. Alexanian, A. P. Balachandran, G. Immirzi and B. Ydri, J. Geom. Phys. **42**, 28 (2002) [arXiv:hep-th/0103023].

[44] A. P. Balachandran, B. P. Dolan, J. H. Lee, X. Martin and D. O'Connor, J. Geom. Phys. **43**, 184 (2002) [arXiv:hep-th/0107099].

[45] J. Medina and D. O'Connor, JHEP **0311**, 051 (2003) [arXiv:hep-th/0212170].

[46] S. Vaidya and B. Ydri, Nucl. Phys. B **671**, 401 (2003) [arXiv:hep-th/0305201].

[47] B. P. Dolan and D. O'Connor, JHEP **0310** (2003) 060 [arXiv:hep-th/0306231].

[48] A. P. Balachandran, S. Kürkçüoğlu and S. Vaidya, arXiv:hep-th/0511114.

[49] C. S. Chu, J. Madore and H. Steinacker, JHEP **0108** (2001) 038 [arXiv:hep-th/0106205].

[50] S. Baez, A. P. Balachandran, B. Ydri and S. Vaidya, Commun. Math. Phys. **208** (2000) 787 [arXiv:hep-th/9811169].

[51] H. Grosse, C. Klimčík and P. Prešnajder, Commun. Math. Phys. **178**, 507 (1996) [arXiv:hep-th/9510083].

[52] A. P. Balachandran and S. Vaidya, Int. J. Mod. Phys. A **16**, 17 (2001) [arXiv:hep-th/9910129].

[53] P. Prešnajder, J. Math. Phys. **41**, 2789 (2000) [arXiv:hep-th/9912050].

[54] U. Carow-Watamura and S. Watamura, Commun. Math. Phys. **212** (2000) 395 [arXiv:hep-th/9801195].

[55] H. Steinacker, Nucl. Phys. B **679** (2004) 66 [arXiv:hep-th/0307075].

[56] W. Behr, F. Meyer and H. Steinacker, JHEP **0507** (2005) 040 [arXiv:hep-th/0503041].

[57] H. Grosse, C. Klimčík and P. Prešnajder, Int. J. Theor. Phys. **35** (1996) 231 [arXiv:hep-th/9505175].

[58] X. Martin, JHEP **0404**, 077 (2004) [arXiv:hep-th/0402230].

[59] F. García Flores, D. O'Connor and X. Martin, PoS **LAT2005** (2006) 262 [arXiv:hep-lat/0601012].

[60] J. Medina, W. Bietenholz, F. Hofheinz and D. O'Connor, PoS **LAT2005**, 263 (2006) [arXiv:hep-lat/0509162].

[61] T. Azuma, S. Bal, K. Nagao and J. Nishimura, JHEP **0407**, 066 (2004) [arXiv:hep-th/0405096].

[62] K. N. Anagnostopoulos, T. Azuma, K. Nagao and J. Nishimura, JHEP **0509**, 046 (2005) [arXiv:hep-th/0506062].

[63] T. Azuma, S. Bal, K. Nagao and J. Nishimura, JHEP **0509**, 047 (2005) [arXiv:hep-th/0506205].

[64] D. O'Connor and B. Ydri, arXiv:hep-lat/0606013.

[65] B. P. Dolan, D. O'Connor and P. Prešnajder, JHEP **0203** (2002) 013 [arXiv:hep-th/0109084].

[66] B. P. Dolan and D. O'Connor, private communication.

[67] Y. Shimamune, Phys. Lett. B **108** (1982) 407.

[68] P. Bleher and A. Its, arXiv:math-ph/0201003.

[69] S. L. Adler, Phys. Rev. D **23** (1981) 2901.

[70] F. R. Brown and T. J. Woch, Phys. Rev. Lett. **58** (1987) 2394.

[71] N. Madras and A. D. Sokal, J. Statist. Phys. **50** (1988) 109.

[72] J. Shao and D. Tu, "The Jackknife and Bootstrap," (Springer, New York, 1995).

[73] I. Montvay and G. Münster, "Quantum Fields on a Lattice", (Cambridge University Press, Cambridge, 1994).

[74] H. Neuberger, Ann. Rev. Nucl. Part. Sci. **51** (2001) 23 [arXiv:hep-lat/0101006].

[75] S. Chandrasekharan and U. J. Wiese, Prog. Part. Nucl. Phys. **53**, 373 (2004) [arXiv:hep-lat/0405024].

[76] A. D. Kennedy and B. J. Pendleton, Phys. Lett. B **156** (1985) 393.

[77] K. Fabricius and O. Haan, Phys. Lett. B **143** (1984) 459.

[78] M. Lüscher and P. Weisz, JHEP **0109** (2001) 010 [arXiv:hep-lat/0108014].

[79] M. Zach, M. Faber and P. Skala, Phys. Rev. D **57** (1998) 123 [arXiv:hep-lat/9705019].

[80] M. Panero, JHEP **0505** (2005) 066 [arXiv:hep-lat/0503024].

[81] G. Racah, "Group Theory and Spectroscopy," (Institute for Advanced Study, Princeton, 1951), p. 74.

[82] A. R. Edmonds, CERN 55 (1955) 26.

[83] H. Grosse, C. Klimčík and P. Prešnajder, Commun. Math. Phys. **185** (1997) 155 [arXiv:hep-th/9507074].

[84] H. Grosse and G. Reiter, Jour. Geom. Phys. **28** (1998) 349 [arXiv:math-ph/9804013].

[85] A. P. Balachandran, S. Kürkçüoğlu and E. Rojas, JHEP **0207** (2002) 056 [arXiv:hep-th/0204170].

[86] R. Petronzio and E. Vicari, Phys. Lett. B **248** (1990) 159.

[87] P. de Forcrand and O. Jahn, arXiv:hep-lat/0503041.

matrix size	g	power in the $l = 0$ channel	matrix size	g	power in the $l = 0$ channel
7	0.02	0.0015564(7)	10	0.02	0.0032149(35)
	0.03	0.0015558(7)		0.03	0.0032125(34)
	0.04	0.0015566(8)		0.04	0.0032135(35)
	0.05	0.0015561(7)		0.05	0.0032200(37)
	0.06	0.0015557(8)		0.06	0.0032195(36)
	0.07	0.0015557(9)		0.07	0.0032160(35)
	0.08	0.0015558(9)		0.08	0.0032168(35)
	0.09	0.0015562(7)		0.09	0.0032155(35)
	0.10	0.0015558(8)		0.10	0.0032136(35)
8	0.02	0.0020297(19)	11	0.02	0.0038745(42)
	0.03	0.0020342(24)		0.03	0.0038762(44)
	0.04	0.0020317(23)		0.04	0.0038748(43)
	0.05	0.0020324(22)		0.05	0.0038784(41)
	0.06	0.0020347(23)		0.06	0.0038810(42)
	0.07	0.0020316(22)		0.07	0.0038789(43)
	0.08	0.0020353(23)		0.08	0.0038744(41)
	0.09	0.0020329(22)		0.09	0.0038754(45)
	0.10	0.0020318(20)		0.10	0.0038749(43)
9	0.02	0.0025539(28)	12	0.02	0.0045497(61)
	0.03	0.0025569(29)		0.03	0.0045572(53)
	0.04	0.0025576(29)		0.04	0.0045611(50)
	0.05	0.0025569(29)		0.05	0.0045514(54)
	0.06	0.0025537(28)		0.06	0.0045532(55)
	0.07	0.0025492(28)		0.07	0.0045575(58)
	0.08	0.0025570(29)		0.08	0.0045539(53)
	0.09	0.0025551(28)		0.09	0.0045602(56)
	0.10	0.0025561(28)		0.10	0.0045512(55)

Table 2: The power in the zero-channel is not affected by the non-commutative anomaly term.

matrix size	l	Reduced χ^2 assuming non-commutative anomaly	Reduced χ^2 assuming no non-commutative anomaly
7	2	0.921	1.287
	3	0.997	3.367
8	2	1.154	1.330
	3	1.293	1.308
9	2	0.895	0.989
	3	0.276	0.391
	4	0.698	0.702
10	2	0.456	0.458
	3	0.421	0.420
	4	0.598	0.599
11	2	0.217	0.221
	3	0.165	0.165
	4	0.143	0.143
	5	0.097	0.101
12	2	0.157	0.157
	3	0.131	0.131
	4	0.120	0.120
	5	0.127	0.127

Table 3: The results of the data analysis appear to be consistent (where the precision is good enough) or at least not in contradiction with the effect predicted by the non-commutative anomaly.

matrix size	λ	r	$\frac{\xi}{\xi_0}$
2	0.636620	0.5	1.05
		1.67	0.99
		-1.67	1.01
		-0.5	1.34
		-0.83	1.45
		-1.17	1.85
		-1.5	2.48
		-1.83	4.97
		-2.17	13.02
		-2.5	29.51
3	2.148592	-2.711	0.936
		-2.824	1.214
		-2.937	1.980
		-3.051	6.198
		-3.164	7.651
		-3.277	24.75
		-3.390	67.12
		-3.503	128.6
		-3.616	441.58
		-3.729	1016.2
15	5.5	-2.2	3.82
		-2.9	4.87
		-3.6	65.6

Table 4: A comparison between the efficiency achieved by our overrelaxation algorithm (ξ) and an algorithm with pure Metropolis updates (ξ_0): the last column gives a rough estimate of the asymptotic value of the ratio between the amounts of CPU-time required by a standard Metropolis algorithm and our overrelaxation algorithm to reduce the square of the error affecting the average value of an observable down to a given value. Here, the observable under consideration is the trace of Φ, which is directly proportional to $c_{0,0}$, and whose exact expectation value vanishes; this observable is highly sensitive to the capability of an algorithm to span the regions corresponding to the minima of the action.

r	$\delta = 0.16$	$\delta = 0.31$	$\delta = 0.46$	$\delta = 0.61$	$\delta = 1.25$
-2.146	0.829	0.686	0.564	0.470	0.253
-2.259	0.825	0.677	0.555	0.459	0.244
-2.372	0.819	0.668	0.546	0.450	0.236
-2.485	0.816	0.661	0.538	0.440	0.228
-2.598	0.811	0.653	0.527	0.429	0.220
-2.711	0.806	0.645	0.517	0.419	0.213
-2.824	0.801	0.638	0.509	0.411	0.205
-2.937	0.798	0.633	0.501	0.404	0.199
-3.051	0.793	0.625	0.493	0.396	0.195
-3.164	0.790	0.619	0.488	0.389	0.190
-3.277	0.786	0.613	0.479	0.383	0.186
-3.390	0.783	0.608	0.475	0.377	0.182
-3.503	0.780	0.603	0.469	0.372	0.178
-3.616	0.777	0.599	0.463	0.366	0.175
-3.729	0.775	0.593	0.459	0.361	0.173
-3.842	0.771	0.590	0.453	0.357	0.169
-3.956	0.769	0.587	0.449	0.353	0.167
-4.069	0.766	0.581	0.444	0.348	0.164
-4.182	0.763	0.578	0.440	0.344	0.161
-4.295	0.760	0.573	0.435	0.340	0.160
-4.408	0.758	0.570	0.432	0.337	0.157
-4.521	0.756	0.567	0.428	0.332	0.155
-4.634	0.754	0.563	0.424	0.329	0.154
-4.747	0.751	0.559	0.421	0.326	0.151
-4.861	0.749	0.556	0.417	0.322	0.150
-4.974	0.746	0.552	0.413	0.319	0.148
-5.087	0.744	0.549	0.410	0.316	0.145
-5.200	0.742	0.546	0.407	0.314	0.144

Table 5: The average acceptance rate $\mathcal{A}$ in the update process, and its dependence on the variation interval width δ and on r (results from runs at $N = 3$ and $\lambda = 2.148592$).

N	λ	r	σ	$\frac{\xi_{\mathrm{g}}}{\xi_{\mathrm{u}}}$
3	0.48	-0.15	0.49	1.00
			1.00	1.00
			1.69	0.99
3	0.48	-0.6	0.49	1.00
			1.00	1.00
			1.69	1.00
3	0.48	-3.0	0.49	1.05
			1.00	1.01
			1.69	1.02
12	0.48	-0.15	0.49	1.00
			1.00	1.00
			1.69	1.01
12	0.48	-3.0	0.49	1.02
			1.00	1.03
			1.69	1.00

Table 6: A comparison of the algorithm efficiency with overrelaxation steps implemented using a gaussian (ξ_{g}) or a uniform (ξ_{u}) symmetric distribution, characterised by the same variance σ^2.